

## Analysis of 2005 Dahuieh (Zarand) aftershock sequences in Kerman province, southeast Iran

Nemati, M.<sup>1\*</sup> and Gheitanchi, M. R.<sup>2</sup>

<sup>1</sup>Ph. D. Student of Geophysics, Earth Physics Department, Institute of Geophysics, University of Tehran, Iran

<sup>2</sup>Professor, Earth Physics Department, Institute of Geophysics, University of Tehran, Iran

(Received: 8 Sep 2007, Accepted: 13 Oct 2009)

### Abstract

In this study, the 2005 Dahuieh (Zarand) locally recorded aftershock sequence has been analyzed. Having the distribution of aftershocks and the source extension, a W-E trending near vertical faulting with an extension of about 15-20 km could be estimated. The rupture causing the powerful Dahuieh earthquake apparently initiated in the modified epicentric area and propagated unilaterally towards the west. The cross section of aftershocks perpendicular to the fault suggests that the aftershocks had a depth range about 20 km, indicating that the seismic activity took place within the upper crust and the seismogenic layer, in this region, which had a thickness not greater than 20 km. The focal mechanism of the main shock and right lateral motion of the Kuh-Bannan fault suggested that the earthquake fault must be reverse and the northern block acted as a hanging wall during the source process of the main shock. The epicentral distribution of aftershocks showed a lack of activity that was interpreted as the modified location of the main shock. Our results are in agreement with waveform modeling. The time frequency pattern of the aftershock decay followed the Kisslinger stretched exponential descending formula.

**Key words:** Dahuieh earthquake; Kerman Province; source parameters; focal mechanism; seismotectonics; Zarand; aftershock

## بررسی زمین لرزه اصلی و پس لرزه های زمین لرزه ۱۳۸۳ داهوئیه (زرند) کرمان، جنوب شرقی ایران

مجید نعمتی<sup>۱</sup> و محمدرضا قیطانچی<sup>۲</sup>

<sup>۱</sup> دانشجوی دکتری ژئوفیزیک، گروه فیزیک زمین، مؤسسه ژئوفیزیک، دانشگاه تهران، ایران  
<sup>۲</sup> استاد، گروه فیزیک زمین، مؤسسه ژئوفیزیک، دانشگاه تهران، ایران

(دریافت: ۸۶/۱۷، پذیرش نهایی: ۸۸/۲۱)

### چکیده

در روز چهارم اسفند ماه ۱۳۸۳ در ساعت ۵:۵۵ دقیقه و ۲۰ ثانیه بامداد (به وقت محلی، شبکه لرزه نگاری مؤسسه ژئوفیزیک دانشگاه تهران) برابر با ساعت ۲:۲۵ دقیقه و ۲۰ ثانیه بامداد (به وقت گرینویچ) زمین لرزه ای با بزرگای  $MW=6.4$  و  $MS=6.5$  و  $mb=6.4$  شرق شهر زرند (رومرکز در روستای داهوئیه برآورد شد، سازمان زمین شناسی و اکتشافات معدنی کشور) در استان کرمان را لرزاند. استان کرمان از دیدگاه لرزه زمین ساختی در ایالت لرزه زمین ساختی ایران مرکزی جای دارد. در این گستره زمین لرزه های تاریخی زیادی در گذشته روی داده است، مانند زمین لرزه ۱۸۶۴ چترود، زمین لرزه ۱۸۹۷ کوهبنان، زمین لرزه ۱۹۱۱ راور و زمین لرزه ۱۹۳۳ بهاباد. رویداد زمین لرزه بم در این گستره در فاصله نزدیک به ۲۰۰ کیلومتری رومرکز زمین لرزه زرند، به اهمیت لرزه ای آن می افزاید. زمین لرزه داهوئیه ۶۱۲ نفر کشته داشت و ۶۰ روستا را ویران کرد. اگرچه این زمین لرزه در پی گسلی نو پدید آمده است، سامانه گسلی کوهبنان با درازای نزدیک به ۳۰۰ کیلومتر، راستای شمال غربی-جنوب شرقی، شیب تند روبه شمال شرقی و سازوکار راستالغز راستگرد خاستگاه این زمین لرزه بوده است. پس لرزه های زیادی با ایستگاه های شبکه موقت و همچنین ایستگاه های لرزه نگاری مؤسسه ژئوفیزیک دانشگاه تهران برداشت و مکان یابی شده اند. در این پژوهش پس لرزه های مکان یابی شده زمین لرزه داهوئیه، پردازش و بررسی شده اند. برای پردازش این پس لرزه ها الگوی سرعتی پرتو P که تاتار و همکاران، (۲۰۰۵) برای زمین لرزه

بم پردازش کرده بودند، به کار گرفته شد. چشمه زمین لرزه با به کارگیری ویژگی‌ها و پراکندگی پس لرزه‌های بهینه مکان‌یابی شده، گسلی با راستای شرقی غربی، با شیب نزدیک به قائم و با درازای نزدیک به ۲۰-۱۵ کیلومتر پیشنهاد شد. برش از پراکندگی پس لرزه‌ها عمود بر راستای گسل نشان می‌دهد که پراکندگی ژرفی آنها بیشینه به ۲۰ کیلومتر می‌رسد، که بر جای گرفتن جنبایی لرزه‌ای در پوسته بالایی و بر اینکه لایه لرزه‌زا در این گستره بیش از این ژرفا ندارد، دلالت می‌کند. همچنین این پراکندگی ژرفی شیب تندی را نشان می‌دهد که ممکن است شیب گسل زمین لرزه‌ای پنداشته شود. سازوکار زمین لرزه اصلی، جابه‌جایی راستگرد گسل کوهبنان و پراکندگی پس لرزه‌ها چنین پیشنهاد می‌کند که گسل زمین لرزه‌ای راندگی، و بلوک شمالی گسل هنگام رویداد زمین لرزه فرادیواره بوده است. پراکندگی پس لرزه‌ها همچنین یک کاف مکانی را نشان داد که این کاف، کانون بهینه شده زمین لرزه اصلی پنداشته شد. نتایج ما با الگوسازی پرتوهای پیکری برای زمین لرزه، سازگاری دارد (حاتمی، ۱۳۸۶). با به کارگیری شتاب‌نگاشت‌های برداشت شده در ایستگاه‌های شتاب‌نگاری شرق و غرب گسل زمین لرزه‌ای، می‌توان گفت که شکستگی زمین لرزه داهوئیه از گستره بهینه شده برای رومرکز آغاز شده و از شرق به غرب به گونه‌ای یک‌سویه گسترش یافته است. سرانجام واپاشی پراکندگی زمانی پس لرزه‌ها از پیوند نمایی بسط داده شده کیسلینگر ( $n(t)=17.04\exp(-0.032t)$ ) پیروی می‌کند.

واژه‌های کلیدی: زمین لرزه داهوئیه، استان کرمان، پارامترهای چشمه، سازوکار، لرزه‌زمین ساخت، زرنده، پس لرزه‌ها

## 1 INTRODUCTION

The southern extension of Kerman seimotectonic sub-province in the southeast of Iran is one of the seismically active regions in the Middle East. Historical reports indicate that several earthquakes with severe destruction and human loss occurred in this region during the past centuries. powerful earthquakes including MS=6.0 Chatroud in Jan. 1864, MS=6.0 the Kuh-Bannan in May 1897, mb=6.7 Ravar in Apr. 1911, mb=6.4 north of Behabad in Nov. 1933, MW=5.9 Gisk in Dec. 1977 and Mw=7.2 Sirch-Golbaft in Aug. 1981 were reported (Ambraseys and Melville, 1982). All of the historical and pre-instrumental earthquakes were related to kuh-Bannan fault system with 300 kilometers length, northeast dipping, right lateral motion and strike slip mechanism. All of these destructive earthquakes caused extensive damage around the 2005 Dahuieh earthquake epicenter in the past. The instrumentally recorded earthquakes as well as the existence of several active faults also suggested that the region had a high potential of seismic activities.

On Feb. 22, 2005 at 02:25:23.9 GMT and 05:55:20.0 local time (United States Geological Survey, USGS, <http://www.usgs.gov>) (Feb. 22, 2005 at 02:25:23.9 GMT and 05:55:20.0 local time (International Institute of Earthquake Engineering and Seismology of Iran, IIEES,

<http://www.iiies.ac.ir>) and Feb. 22, 2005 at 02:25:23.9 GMT and 05:55:20.0 local time (Institute of Geophysics University of Tehran, IGUT, <http://www.igut.ut.ac.ir>) a shallow destructive earthquake without any felt foreshock occurred near Dahuieh, around Kerman city, in southeast Iran. Like other large earthquakes in southeast Iran, which are often associated with well recognizable surface faulting, this earthquake was accompanied by a clear surface rupture (Talebian, et. al., 2005). The epicentral region, given by USGS, was located near Dahuieh in the Zarand area (30.76N and 56.74E). The magnitudes of the main shock were mb=6.4, MS=6.5 and MW=6.4 and the focal depth was 30 kilometers. Using aftershock distribution, the epicenter of the main shock was modified in the north of the rupture. The main shock which was located near the city of Zarand, severely damaged about 60 villages including Darbidkhoun and Hotkan (near Dahuieh), killed 612 people and destroyed 7000 homes (Geological Survey of Iran, GSI, [http://www.gsi\\_iran.org](http://www.gsi_iran.org)). Maximum intensity (IEES) of the main shock exceeded VIII on the Modified Mercalli Intensity (MMI) scale (Fig. 1).

Shortly after occurrence of the main shock, the Geophysics Institute of University of Tehran deployed a temporary seismic network in the damaged area and monitored the aftershock activities. This paper analyzes

the locally recorded aftershock activity and compares it with the results of the Geological studies. First, the seismotectonics setting of the region is reviewed. Then, the source parameters of the main shock and the strong aftershocks are explained. Finally, the result of locally recorded aftershocks is presented and discussed.

## 2 SEISMOTECTONICS SETTING

Central Iran is limited by the Great Kavir Fault in the north, the Nehbandan fault in the west and the Nain-Dehshir-Baft fault system in the southwest. Kerman seismotectonic sub-province is located in Posht-e-Badam block, one of the central Iran blocks. There are Pre-Cambrian metamorphic outcrops in this block (Aghanabati, 2005). There are many strike slip motion, right lateral mechanism and NW-SE strike faults like Kuh-Bannan, Ravar, Nayband, Lakar-kuh and Rafsanjan faults. Along the south of the

Posht-e-Badam block there is a major NW-SE to N-S trending right-lateral fault system. The Kuh-Bannan is a major active fault with northeast dipping in this system which impressed the Dahuieh earthquake rupture. The right-lateral motion along this fault, 5 (mm/year) (Talebian, et. al., 2005), has created secondary, reverse, north dipping faults, like the Dahuieh rupture, in the east side. From geological maps of the Dahuieh area (GSI) and aftershock location, it is clear that the coseismic rupture occurred in the shale and sandstone of the Nayband formation. The strike of rupture must follow the layering in sandstone and shale. Figure 1 shows the map of the main faults, epicenters of instrumental and historical earthquakes, focal mechanism, occurrence date of the significant events in the Dahuieh area and iso-seismal curves of the Dahuieh earthquake.

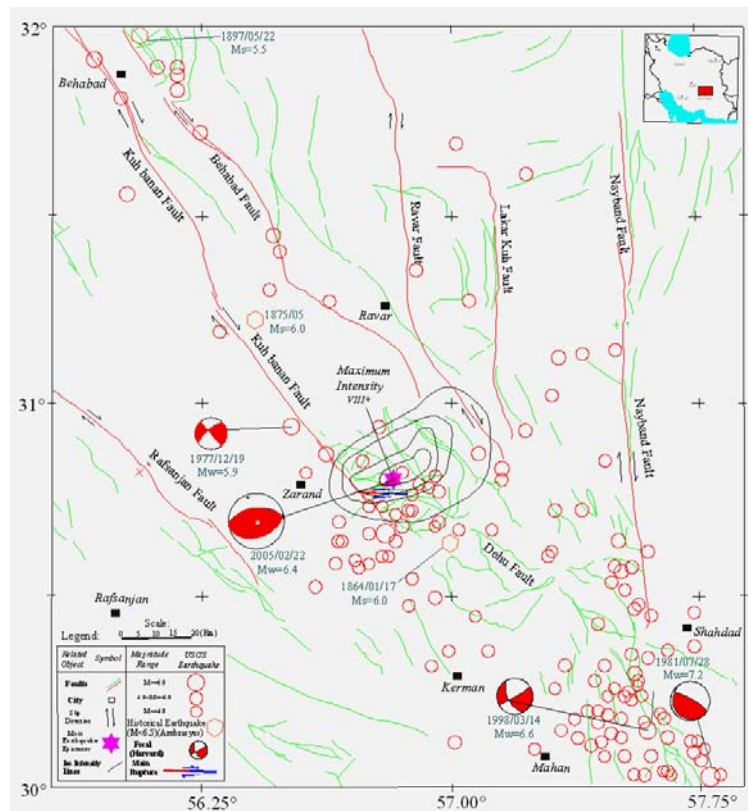


**Figure 1.** The map of main (red lines) and minor (green lines) faults (GSI 1:250,000 Geological maps), epicenter of instrumental (USGS) and historical (Ambraseys), focal mechanism (Harvard), occurrence date of important earthquakes in the Kerman area and isoseismal curves (IIEES) of the Dahuieh earthquake. Open red circles show instrumental, polygons show pre-instrumental and historical earthquakes, the star shows the epicenter of the Dahuieh main shock and solid rectangles show neighboring cities.



All of the main faults, as shown in the map, have right-lateral and strike-slip motion. Fig. 2 shows the map of isoacceleration and two near accelerograms recorded by the accelerometers in the west and the east of rupture of the Dahuih earthquake. As shown in the map maximum acceleration, created by this earthquake, exceeds 300 millimeters per square second (Building and House Research Center, BHRC, <http://www.bhrc.ac.ir>).

### 3 SOURCE PARAMETERS OF THE MAIN SHOCK AND SIGNIFICANT AFTERSHOCKS

The main shock was followed by many strong aftershocks (Fig. 3), which caused additional damage and destruction in the affected area. Aftershock processing was done using the records of 24 IGUT permanent stations and 5 temporary short

period seismic stations. The epicenter of the main shock was modified as 30.80N and 56.84E and a depth of 9 km (Figure 4a) (Nemati, 2006). The depth of the main shock is in agreement with waveform modeling conclusions (Talebian, et. al., 2005). From 5 seconds S minus P travel time using S and P arrival times of Zarand accelerograph (Fig. 2), it is calculated about 25 Km epicentral distance from the Zarand station which corresponds to the modified epicenter. The recorded aftershock sequence indicates that the strongest aftershock, with  $m_b=4.4$ , occurred four days after the main shock. The Harvard centroid moment tensor solution of the main shock indicates pure reverse with a small component of right-lateral strike-slip mechanism. Table1 shows the source parameters of the Zarand main shock and its significant aftershocks.

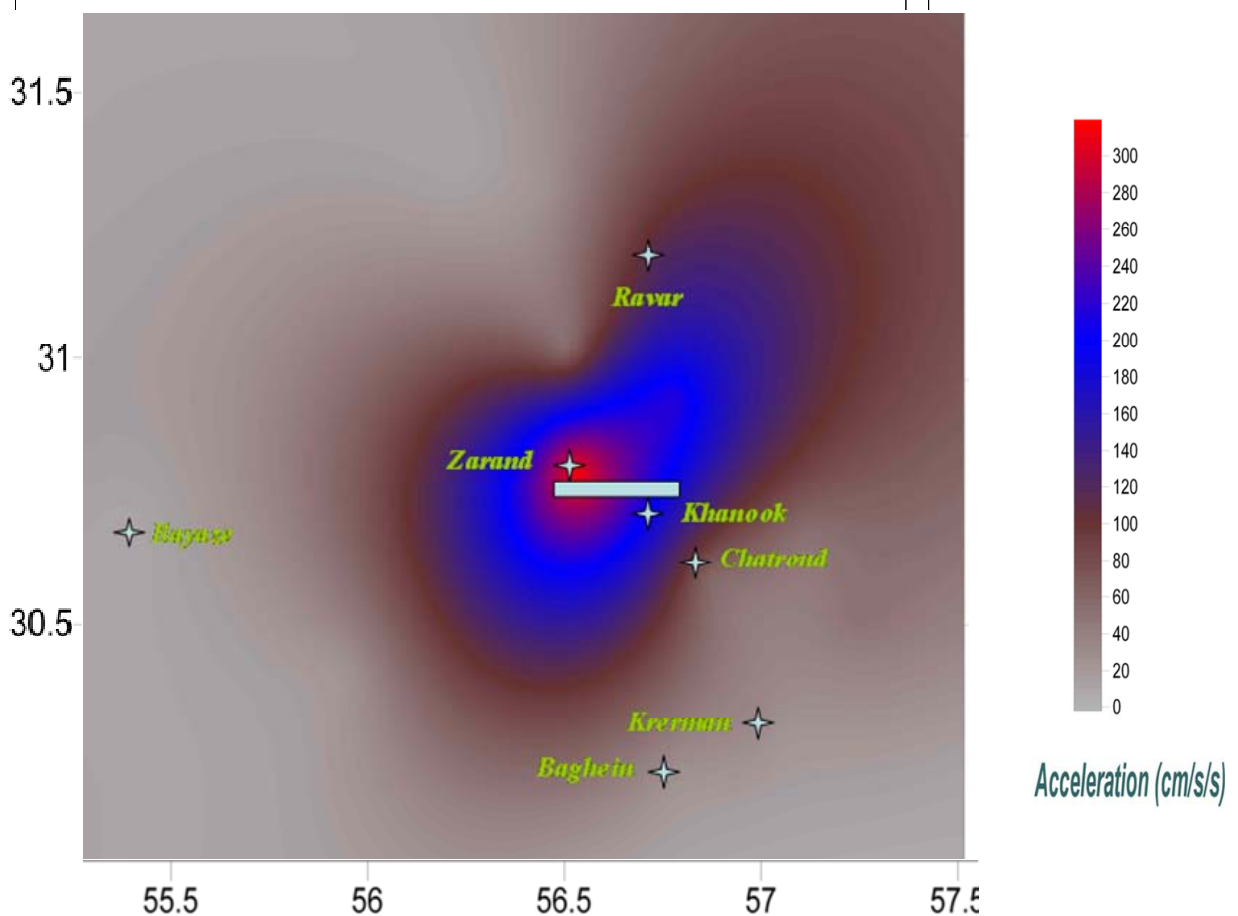


**Figure 2.** The map of iso-acceleration and nearest accelerometers (Star) (BHRC). The thick green line is the rupture from Talebian, et al., (2005).



#### 4 LOCALLY RECORDED AFTERSHOCK SEQUENCE

To study the aftershock activities in detail, a temporary seismic network was deployed in the affected area one day after the occurrence of the main shock, and recorded the activities for about two months. The recorder instruments were five Portable Digital Acquisition Systems (PDAS-100). The PDAS recorders were recorded at a sampling rate of 50 samples per second and the detection level was so that the events with magnitude greater than 1.5 could be detected and located. We located about 400 aftershocks that were recorded by at least five stations. We used the  $V_p/V_s$  ratio given by Tatar, et al., (2005), for 2003 MW=6.6 Bam earthquake at a distance about 200 kilometers from Dahuieh. We examined several crustal models and applied the best one which is made of a layer of 11 km with a velocity  $V_p=5.0$  km/s, over a layer of 8 km with a velocity  $V_p=5.9$  km/s over a layer of 29 km with a velocity  $V_p=6.5$  km/s, over a half-space with  $V_p=8.1$  km/s. The aftershocks were processed using HYPO71 program (Lee and Valdes, 1985) and the best located of them were selected on the basis of RMS smaller than 0.2 s, azimuthal gap smaller than  $180^\circ$ , number of read phases for locating, greater than 7, horizontal and vertical errors of location smaller than 2 km. Depth distributions of the aftershocks is shown in Figure 4a. The green line in this figure shows the depth rupture estimated by the dispersal of the aftershocks and M.S. indicates the main shock focus. Linear accumulation of a few aftershocks at a depth of 15 km comes from initial depth for locating during processing with HYPO71 software.

Aftershock activities appeared to be close to the macroseismic epicenter having focal depths down to 20 km (Fig. 4a). This indicates that the faulting was mainly initiated and taking place in the upper crust beneath the sedimentary covers. Parameters of about 400 aftershocks were determined but only 140 well located ones were used for this analysis. For the well located aftershocks the

error in the focal depth determination is less than 2 km. The location of seismic stations and the epicentral distribution of well located aftershocks as well as the related surface ruptures are shown in Figure 3. Aftershocks extended over a zone approximately 15-20 km in length with a general W-E elongation. We calculated 15 km source dimension using the following famous formula (1) with  $M_0=5.05 \times 10^{25}$  N.m (USGS),  $\alpha=5 \times 10^{-5}$  and  $\mu_0=3 \times 10^{10}$  Nm<sup>2</sup>.

$$L^3 = M_0/\alpha\mu_0 \quad (1)$$

Figure 3 shows the distribution of well located to aftershocks related coseismic rupture and temporary stations. The sparse density distribution region of the aftershocks (region of main shock) is related to the surface rupture and their high density distribution region is coupled with the blind rupture.

#### 5 EMPIRICAL RELATIONS FOR THE RATE OF AFTERSHOCK DECAY

Time frequency pattern of the aftershocks generally indicates that the activity was very intensive immediately after the main shock occurrence. As shown in Figure 4b the number of events decreased significantly during the first days. There are several empirical relations for the rate of aftershock decay (Christophersen and Smith, 2000; Yamashita, Knopoff, 1987). For this region the stretched exponential function (2), (Kisslinger, 1993), is suggested.

$$n(t)=a+b*\exp(-t/c)^q \quad (2)$$

The  $n(t)$  is the frequency of aftershocks per time  $t$  following the main shock and  $a$ ,  $b$ ,  $c$  and  $q$  are constants and should be determined for each region.

As shown in Figure 4b our aftershock decay follows the stretched exponential descending formula (3), in which  $a=0$ ,  $b=17.04$ ,  $c=1/0.032$  and  $q=1$ . The red curve in Figure 4b is the best fitted curve for aftershock decay using the least square method.

$$n(t)=17.04\exp(-0.032t) \quad (3)$$



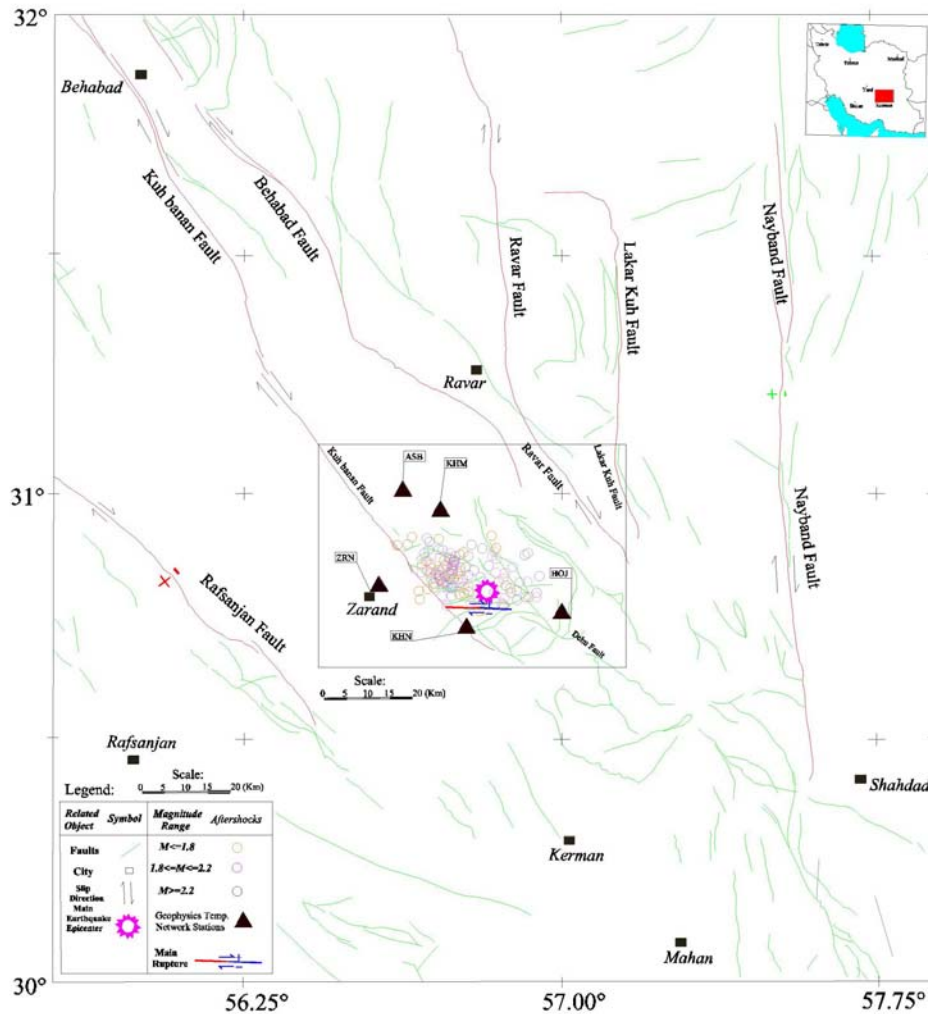


**Figure 3.** Distribution of well located aftershocks. The blue part of the main rupture is the surface rupture and the red part is the blind rupture (Talebian, et al., 2005). There is agreement between the aftershock distribution and modified location of the mainshock. Blue circles show aftershocks with magnitudes greater than 2.2.

**Table1.** Source parameters, date, time, latitude, longitude, depth, magnitude, RMS and their references, for Zarand significant aftershocks and date, time, latitude, longitude, depth, moment, strike, dip, slip, magnitude and their references, for the main shock. As shown in the table, the strongest aftershocks occurred shortly after the main shock. Date, time, moment,  $M_w$ , strike and slip of the main shock are from Harvard University and USGS. Lat., long. and depth of main shock and dipping of the fault have been modified by aftershock distribution and aftershock magnitudes are in mb scale.

Date	Time	Lat.°	Long.°	Depth(Km)	M(N.m)	$M_w$	Strike	Dip	Slip	RMS	Ref.
2005 Feb. 22	2:25:22	30.77	56.74	7	-	6.4	270	60	104	-	*
2005 Feb. 22	2:25:24	30.80	56.84	5			266	38	106	-	**
2005 Feb. 22	2:25:24	30.80	56.84	8	$5.05 \times 10^{25}$	6.4	261	80	97	-	here <sup>1</sup>
2005 Feb. 23	17:36:11	30.87	56.78	3	-	4.0	-	-	-	0.16	here
2005 Feb. 24	23:26:30	30.84	56.70	15	-	4.1	-	-	-	0.12	here
2005 Feb. 25	1:11:58	30.82	56.76	14	-	4.1	-	-	-	0.17	here
2005 Feb. 25	19:54:15	30.62	56.55	2	-	4.1	-	-	-	0.16	here
2005 Feb. 26	9:09:53	30.72	56.85	15	-	4.4	-	-	-	0.01	here
2005 Feb. 27	13:20:45	30.79	56.74	4	-	4.2	-	-	-	0.07	here

(\*Talebian, et al., 2005)(\*\*Hatami, 2007)

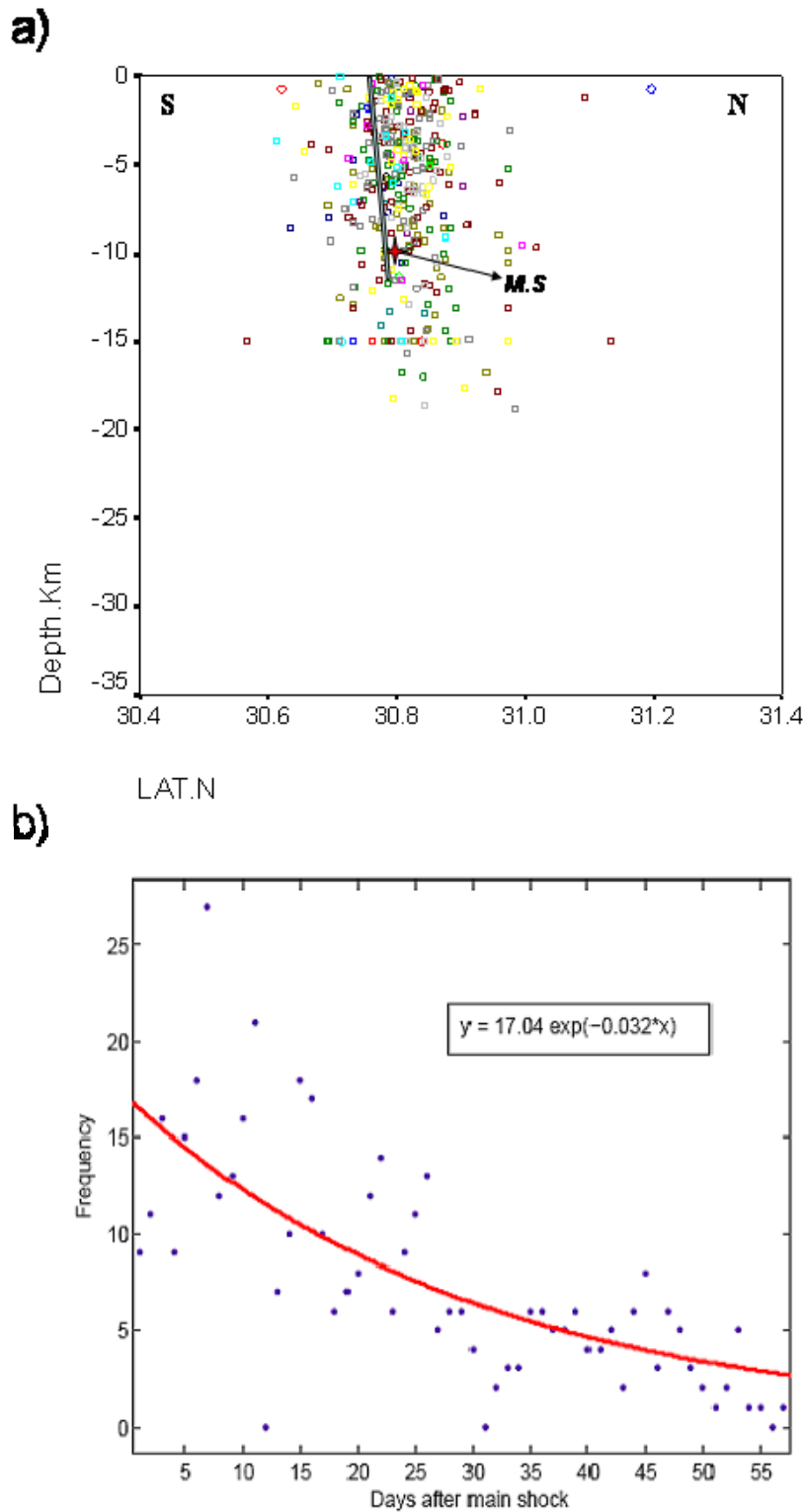


**Figure 4.** a) The N-S cross section shows distribution of the aftershocks with fault plane estimation in depth. b) The time frequency diagram of the aftershock decay.

## 6 DISCUSSION AND CONCLUSIONS

The distribution of the locally recorded aftershocks revealed that the majority of aftershocks were located on the northern block and the fault trace acted as a delimiting line. This suggests that the northern block acted as a hanging wall during the source process of the main shock. From the spatial distribution of aftershocks and the cross section perpendicular the main surface faulting, an area with lack of locally recorded aftershock activities is seen (fig.4a). The observed lack of aftershock activities could be the modified main shock location. This is in agreement with conclusions of modeling of seismic body waves, radar interferometry and field investigation (Talebian, et. al., 2005) for depth calculation of the main shock. Table 1 is a clear comparison between the parameters deduced from aftershock activities and other work.

The along of aftershocks on the cross section across the main fault trend suggests that the fault plane should be nearly vertical. Considering the epicenter of the main shock as the initial break and comparing two nearest accelerographs in the west and the east of the rupture and the distribution of the locally recorded aftershocks compared with the epicenter of the main shock indicates that the rupture was initiated in the east and extended to the west in a unilateral manner. This fact could also be understood from the location of the main shock and the extension of the surface rupture. The extent of aftershock activities and source dimension calculation indicates a range of 15-20 km source dimension, and is in agreement with the observed surface rupture. The vertical cross-section across the main ruptured trend reveals that the aftershocks were distributed within a depth range of 20 km with the highest density around the depth of 6 km. This suggests that the faulting is mainly blind and took place in the uppermost basement beneath the sedimentary covers (blind rupture is greater than surface rupture). It is concluded that the seismic activity is taking place within the upper crust and the seismogenic layer, in this region, has a

thickness not greater than 20 km. The time frequency pattern of aftershock decay follows the Kisslinger stretched exponential descending formula. The extension of the aftershock activity indicates a diffused pattern and lower depth than the main shock. This could be related to the complex fault system and tectonics in this region.

## 7 ACKNOWLEDGEMENTS

We are grateful to the Geophysics Institute of Tehran University for giving the waveform of aftershocks.

## REFERENCES

- Aghanabati, A., 2005, Iran Geology, Geological Survey of Iran (Persian book).
- Ambraseys, M. and Melville, C. P., 1982, A History of Persian Earthquakes [M]. Lonsn: Cambridge University Press, 219.
- Berberian M., 1976, Contribution to the seismotectonics of Iran (part 2) [J]. Rep Geol. Surv. Iran, 39,516.
- Christophersen, A. and Smith, E. G., 2000, A Global Model for Aftershock Behavior, 0739, 12WCEE, 2000.
- Hatami, M. R. 2007, Computing of mechanism of the 2005 Feb. of Dahuieh (Zarand) based on amplitude spectrum of waves and polarities. Journal of Earth and Space Physics, 33, No. 1386-3, 35-46.
- Kisslinger, K., 1993, The Stretched Exponential Function as an Alternative Model for Aftershock Decay Rate. JGR Vol.98, No. B2, 1913-1921.
- Lee, W. H. K. and Valdes, C. M., 1985, HYPO71PC: A personal computer version of the HYPO71 earthquake location program [R]. U S Geol. Surv., Open File Report, 85-749, 43.
- Nemati, M, 2006, Analysis of 2005 Feb.22 Dahuieh (Zarand) Earthquake [D] [MS Thesis] (in Farsi), University of Tehran.
- Tatar, M., Hatzfeld, D., Moradi, A-S. and Paul, A., 2005, The 2003 December 26 Bam earthquake (Iran), Mw=6.6 aftershock sequence Geophys. J. Int., 163, 90-105.
- M. Talebian, J. Biggs, M. Bolourchi1, A. Copley, A. Ghassemi, M. Ghorashi, J.

- Hollingsworth, J. Jackson, E. Nissen, B. Oveisi, B. Parsons, K. Priestley, A. Saiidi, 2005, The Dahuiyeh (Zarand) earthquake of 2005 February, 22 in central Iran. *Geophys. J. Int.*, 164, 137-148.
- Yamashita, T. and Knopoff, L., 1987, Models of aftershock occurrence, *Geophysics J. Soc.*, **91**, 13-26.